Triggering of destructive earthquakes in El Salvador

José J. Martínez-Díaz
José A. Álvarez-Gómez — Departamento de Geodinámica, Universidad Complutense de Madrid, Madrid 28040, Spain
Belén Benito E.U.I.T., Topografía, Universidad Politécnica de Madrid, Madrid 28031, Spain
Douglas Hernández Servicio Nacional de Estudios Territoriales, Avda Las Mercedes, San Salvador, El Salvador

ABSTRACT

We investigate the existence of a mechanism of static stress triggering driven by the interaction of normal faults in the Middle American subduction zone and strike-slip faults in the El Salvador volcanic arc. The local geology points to a large strike-slip fault zone, the El Salvador fault zone, as the source of several destructive earthquakes in El Salvador along the volcanic arc. We modeled the Coulomb failure stress (CFS) change produced by the June 1982 and January 2001 subduction events on planes parallel to the El Salvador fault zone. The results have broad implications for future risk management in the region, as they suggest a causative relationship between the position of the normal-slip events in the subduction zone and the strike-slip events in the volcanic arc. After the February 2001 event, an important area of the El Salvador fault zone was loaded with a positive change in Coulomb failure stress (>0.15 MPa). This scenario must be considered in the seismic hazard assessment studies that will be carried out in this area.

Keywords: seismic triggering, seismic hazard, stress transfer, active tectonics, El Salvador.

INTRODUCTION

El Salvador has suffered at least 11 destructive earthquakes during the past 100 yr (see Data Repository for data[1]). These events caused more than 3000 deaths because of the effects of shaking and/or the subsequent landslides (White and Harlow, 1993; Bommer et al., 2002). The seismically active area of El Salvador is close to the Cocos-Caribbean segment of the Middle American subduction zone, where the plates converge with velocities of 73–84 mm·yr^{-1} (DeMets, 2001) (Fig. 1). Two different types of earthquakes—distinguished by their tectonic origin and location—occur in this area. The largest earthquakes (M_w >7.0) are generated in the subducted Cocos plate and along its interface with the Caribbean plate (Dewey and Suarez, 1991). They rupture at intermediate depths (~200 km), producing slight damage. In the continent, the faults along the volcanic arc generate moderate-magnitude ($5.5 < M < 6.8$), upper-crustal ($h < 20$ km) earthquakes (White, 1991) (Fig. 1) that are responsible for most of the damage and destruction.

These differences in seismic activity are driven by the process of strain partitioning proposed by Harlow and White (1985) and supported by geodetic observations (DeMets, 2001). The moderate-sized, upper-crustal earthquakes accommodate trench-parallel strike-slip motion (White et al., 1987). The largest and deepest subduction earthquakes result from two different mechanisms: thrusting along the Wadati-Benioff zone, and normal faulting due to extensional forces generated by slab-pull forces or bending of the subducting plate (Isacks and Baranzagi, 1977).

The large normal-slip earthquakes that ruptured in the subducting plate close to the El Salvador coast (1982, M_s 7.3; and 2001, M_s 7.8) were preceded and followed by destructive strike slip events in the volcanic arc (1951, M_s 5.9; 1965, M_s 6.3; 1986, M_s 5.4; 2001, M_s 6.5). The possibility that this succession was related to coseismic and postseismic interactions between different earthquakes has been proposed (Parsons, 2002; Benito et al., 2004). The transfer of the Coulomb failure stress (CFS) produced during a main shock is able to induce other main shocks and/or control the location of aftershocks, even at tens of kilometers (King et al., 1994; Harris, 1998; Stein, 1999). Parsons (2002) modeled the transference of static stress on ideally oriented planes to analyze the

[1]GSA Data Repository item 2004010, table of earthquake parameters, map of earthquakes and modeling of surface ruptures, is available at www.geosociety.org/pubs/ft2004.htm, or on request from editing@geosociety.org or Documents Secretary, GSA, P.O. Box 9140, Boulder, CO 80301-9140, USA.

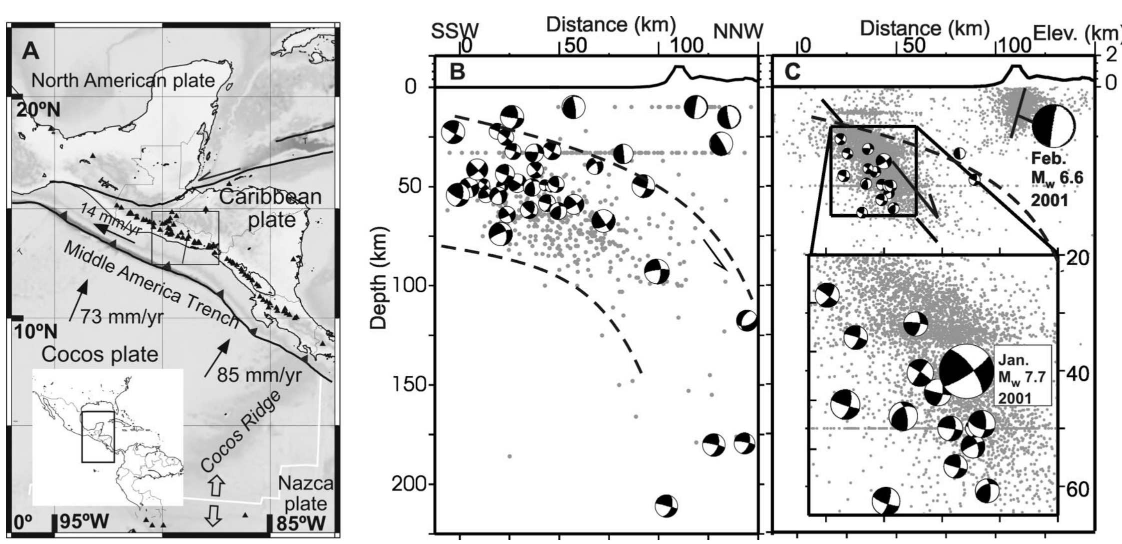

Figure 1. A: Geodynamic setting of study area. Line within box indicates trace of cross sections B and C. Plate motion direction and rates are shown by arrows (data from DeMets, 2001). B: Cross section passing through coordinates 13.93°N, 88.78°W. Focal mechanisms were taken from Harvard Centroid Moment Tensor (CMT) and U.S. Geological Survey–National Earthquake Information Center (USGS-NEIC) catalogues (period 1977–February 2003). Gray dots are hypocenters from USGS-NEIC database (M_s >2.5). Dashed lines represent estimation of upper and lower bounds of seismogenic zone of subducted slab. C: Cross section of 2001 seismic sequence of El Salvador following two main shocks of January and February. Hypocenters are from Servicio Nacional de Estudios Territoriales catalogue and focal mechanisms are from Harvard CMT and USGS-NEIC catalogues.

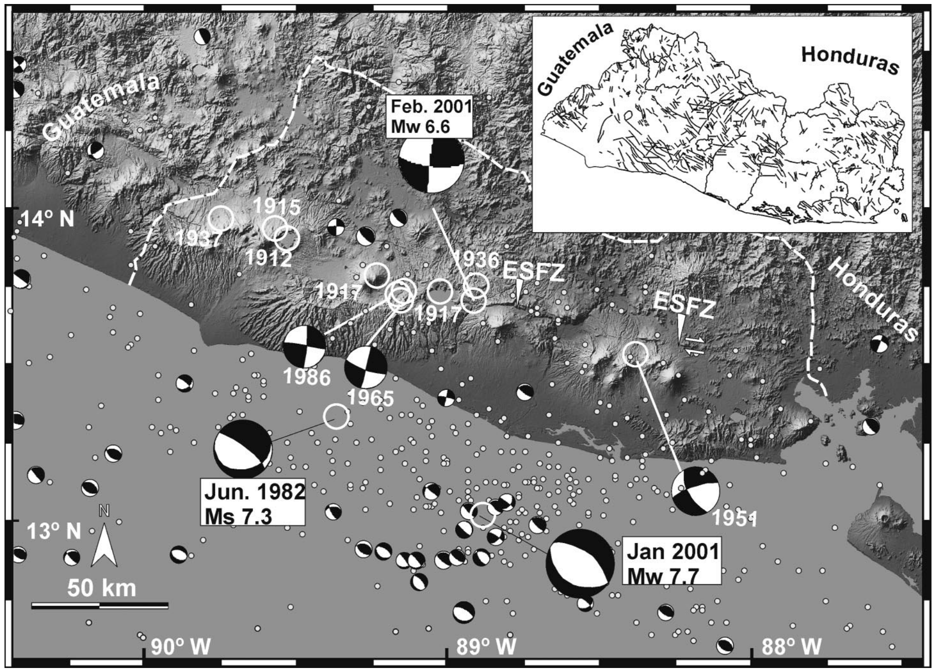

Figure 2. Radar–Shuttle Radar Topography Mission image of El Salvador (courtesy of Jet Propulsion Laboratory) with historical destructive earthquakes (white circles) and instrumental epicenters (M_s >2.5, period 1977–2001) from U.S. Geological Survey–National Earthquake Information Center (USGS-NEIC) catalogue (small dots). Small focal mechanisms are from events with M_w >5.5 (period 1977–2001, Harvard Centroid Moment Tensor database). Large mechanisms are from Buforn et al. (2001). Inset: map of faults extracted from *Geological Map of El Salvador* (Bosse et al., 1978). ESFZ—El Salvador fault zone.

possibility that the subduction-related earthquake of January 2001 triggered the earthquake of February 2001 in the volcanic arc. The lack of good-quality seismic data prevented the utilization of the failure planes and limited the conclusions of that study.

New seismological and seismotectonic data allow us to model the change of Coulomb failure stress on planes selected with geologic criteria. We investigate the geologic source of the major earthquakes in the volcanic zone by using earthquake locations, focal mechanisms, and geomorphic expression of faults. Using this information, we performed several models of static Coulomb stress transfer induced by the 1982 and 2001 shocks.

SEISMIC ACTIVITY IN EL SALVADOR

The earthquake locations data used in the temporal and spatial analysis come from several sources: the historic earthquake data were obtained from the catalogue of White and Harlow (1993) and from Bommer et al. (2002), and the instrumental seismicity data for the 1973–2001 period were taken from the U.S. Geological Survey (USGS)–National Earthquake Information Center (NEIC) catalogue. For the 2001 period we used the catalogue of earthquakes relocated by the SNET (Servicio Nacional de Estudios Territoriales); the focal mechanisms are from the Harvard and USGS-NEIC Centroid Moment Tensor (CMT) databases and from Buforn et al. (2001).

The 11 destructive earthquakes that took place in the twentieth century are significantly aligned along the volcanic arc (Fig. 2). On 8 June 1917, an M_s 6.4 earthquake occurred 30–40 km west of the San Salvador volcano, followed 30 min later by an M_s 6.3 earthquake. In 1919, an M_s 6 earthquake occurred, the epicenter of which was situated at about the same location of an earthquake in 1986. Four reliable focal mechanisms are available for the more recent major events of 1951, 1965, 1986, and 2001. They are all strike-slip events with one of the planes oriented east-west, parallel to the volcanic arc. The San Salvador earthquake of 10 October 1986 originated on the volcanic arc and propagated along a nearly vertical, north-northeast–striking plane close to San Salvador (White et al., 1987). However, the largest earthquakes in the area (1982 and 2001) occurred in the subduction zone and have almost identical normal-slip mechanisms with planes oriented N120°–130°E.

The 2001 seismic sequence is especially interesting because of the large catalogue of well-located aftershocks that has been used to model the surface rupture both in the subduction (13 January) event (M_w 7.7) and in the volcanic arc (13 February) earthquake (M_w 6.6). The spatial analysis of the aftershocks (see footnote 1) that occurred during the three days following the main shocks gives, for the January event, the best-fit solution, with a plane dipping 60°NE and a N128°E strike, subparallel to the Middle America Trench (Fig. 1) and is consistent with the focal mechanism calculated by Buforn et al. (2001). The fault has a rupture area of 2532 km^2 (60 × 42 km). By using teleseismic, regional, and local data, Vallée and Bouchon (2003) modeled this rupture area and obtained a plane with the same orientation. For the crustal earthquake of 13 February the best-fit solution indicates a rupture sized 471 km^2 (40 × 12) striking N94°E and dipping 70°S (Fig. 2).

EL SALVADOR FAULT ZONE

The map of faults extracted from the *Geological Map of El Salvador* (scale 1:100,000; Bosse et al., 1978) shows the existence of three sets of faults that strike northwest, north-northeast, and east, and are distributed throughout the region (Fig. 2). Most of these faults are <30 km long. The north-northeast– and east-striking faults are parallel to the orientation of the plane solutions of the focal mechanisms. The C-band interferometric radar image from the Shuttle Radar Topography Mission (Jet Propulsion Laboratory, National Aeronautical and Space Administration: http://photojournal.jpl.nasa.gov/) and the digital elevation model built from 1:25,000 scale topographic maps (Fig. 3) show the existence of a large structure, >100 km long, that we have called the El Salvador fault zone (Fig 2). This fault zone, which is oriented N90°–100°E, is composed of several structural segments and extends from the eastern border of El Salvador to the western side of Lago Ilopango.

The El Salvador fault zone deforms Quaternary deposits with right-lateral and oblique-slip movements. These movements are evident when the fault affects the acid pyroclastic rocks of the Tierra Blanca and Tobas Color Café Formations. The topographic expression of this fault zone shows that right-lateral movement has deflected the Rio Lempa, the Rio Grande de San Miguel, and the fluvial network northwest of Jucuapa (Fig. 2). The western part of the El Salvador fault zone passes near the city of San Vicente and cuts both the northern slope of the San Vicente volcano and the Lago Ilopango depression.

Six of the major destructive earthquakes along the volcanic arc occurred on the western part of the El Salvador fault zone. The distribution of aftershocks following the February 2001 (M_w 6.6) earthquake shows clearly that this event was produced by the rupture of a segment of the fault zone from Rio Lempa to Lago Ilopango (RS in Fig. 3). In summary, the local geology supports that the segments of the El Salvador fault zone are the sources

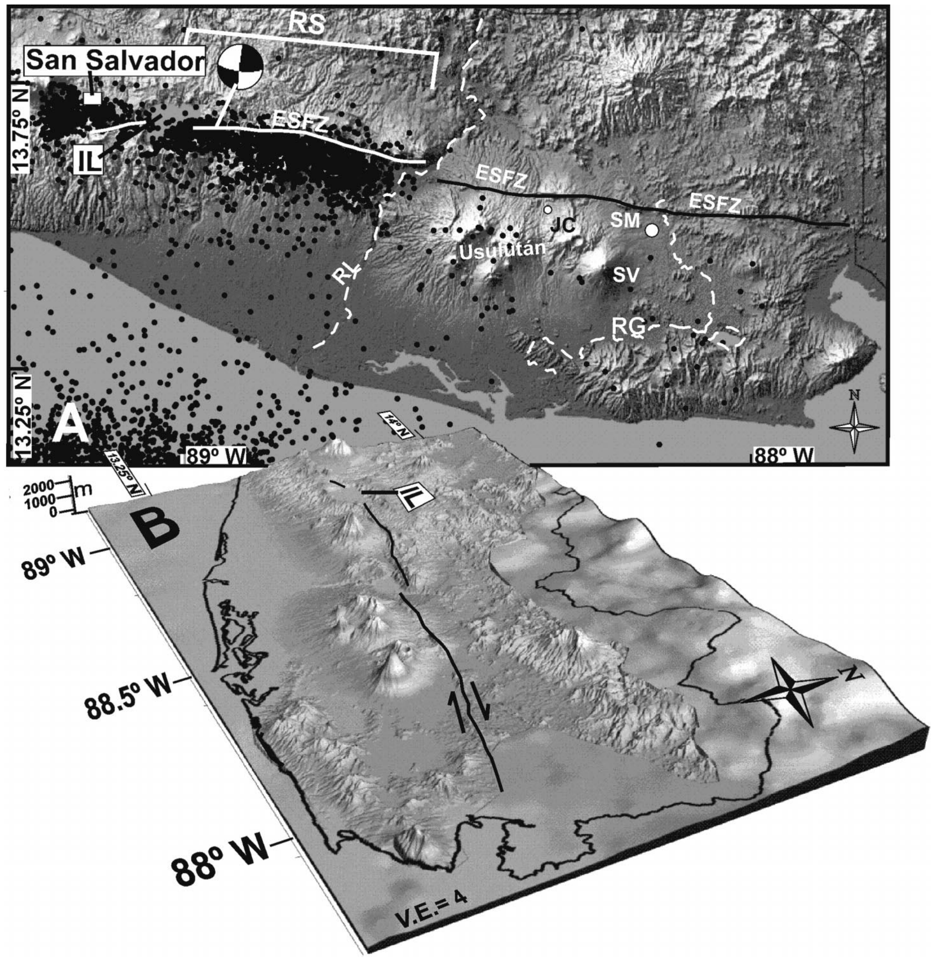

Figure 3. A: Aftershocks sequence of February 2001 (M_w 6.6) event projected on Radar image of El Salvador fault zone (ESFZ). SM—San Miguel; SV—San Miguel volcano; IL—Lago Ilopango; RS—rupture segment; JC—Jucuapa; RL—Rio Lempa; RG—Rio Grande. B: Oblique view of digital elevation model of volcanic arc with ESFZ trace.

of the destructive earthquakes along the volcanic arc.

STRESS-TRANSFER MODELING

To calculate how the large, subduction-related earthquakes can affect the stability of the El Salvador fault zone, we modeled the static stress change generated by the 1982 and 2001 earthquakes on planes parallel to that fault zone. These planes are also parallel to the focal solution of the 1986 (M_w 5.7) and February 2001 (M_w 6.6) earthquakes. We have estimated the change in the Coulomb failure stress (ΔCFS) by the equation $\Delta CFS = \Delta\tau_\beta - \mu'\Delta\sigma_\beta$, where $\Delta\tau_\beta$ is the change in shear stress on a receiver fault, $\Delta\sigma_\beta$ is the change in normal stress acting on the receiver fault, and μ' is the apparent coefficient of friction, and includes the effects of pore fluid and the material properties of the fault zone (see Harris, 1998). The positive values for ΔCFS promote faulting, whereas negative values inhibit the activity. We have estimated the stress change in an elastic half-space using the GNStress code and following the Okada (1992) method. The apparent friction coefficient is taken as 0.4, which is an acceptable value, as proposed by Deng and Sykes (1997). In any case, the introduction of different values for the apparent frictional coefficient did not produce significant changes in the results.

The fault geometry and slip directions used in the models are derived from the focal mechanisms (Table 1) and from a spatial analysis (see footnote 1) of the aftershocks described in detail in Benito et al. (2004). The ruptures were modeled as rectangles with the slip tapered on the rectangular slip patches. The results in Figure 4 show the CFS change (ΔCFS) in map view projected to the hypocentral depth of the October 1986 and February 2001 events. The model for the 2001 event is also shown in cross section. Both models indicate that the earthquakes of the volcanic axis occurred in segments of the El Salvador fault zone where the change in CFS goes beyond 0.1 MPa. The majority of the aftershocks of the February 2001 earthquake occurred in the zone of CFS increase. Shallow aftershocks with $M_s > 3.0$ following the February 2001 event occurred in the lobes of CFS increase on the El Salvador fault zone (Fig. 4C).

CONCLUSIONS

The models show that normal-slip earthquakes in the subduction area induce a lobe of CFS increase on steeply dipping N90°E planes in the volcanic axis zone. These kinds of earthquakes generate CFS increases of as much as 0.3 MPa in a wide area of the seismogenic zone of the El Salvador fault zone. Reverse-slip earthquakes linked to subduction along the Wadati-Benioff zone and situated at the same distance as the modeled normal-slip events were also modeled, and the results show CFS decreases in the El Salvador fault zone.

The pattern of CFS change induced by the three greatest shallow earthquakes that occurred in the study area since 1982 on planes parallel to the El Salvador fault zone (Fig. 4E) suggests a causative relationship between the normal-slip events in the subduction zone and the strike-slip events in the volcanic arc. Moreover, the CFS map shows that after the February 2001 event an important area of the El Salvador fault zone to the east of the Rio Lempa has been loaded with a positive change in Coulomb failure stress (>0.15 MPa) (Fig. 4E). A large hypothetical extensional event located to the southeast of the January 2001 event would produce a CFS reload in that area that would promote seismic activity in the fault zone. The location of the next large extensional earthquake must be considered in the evaluation of the probabilities of shaking and expected accelerations along the volcanic area.

A more complete modeling study including all the events with magnitude M_w >5.0 is nec-

TABLE 1. PARAMETERS USED IN COULOMB FAILURE STRESS MODELS GENERATED BY THE THREE LARGEST EVENTS STUDIED

Event date D/M/Y	Plane			Center of rupture		M_w	D_T (km)	Rupture area (km)
	Dip direction	Dip	Rake	Lat (°N)	Long (°W)			
13/02/2001	184°	70°	−180°	13.67	−88.94	6.6	5	42 × 12
13/01/2001	30°	60°	−98°	13.1	−88.9	7.7	20	60 × 42
19/06/1982	29°	66°	−82°	13.29	−89.39	7.3	20	50 × 35

Note: D_T = depth to the top of the rupture. Rupture dimensions for 2001 earthquake are taken from the spatial analysis of aftershocks. For the 1982 earthquake, the dimensions are estimated by using the equations of Wells and Coppersmith (1994).

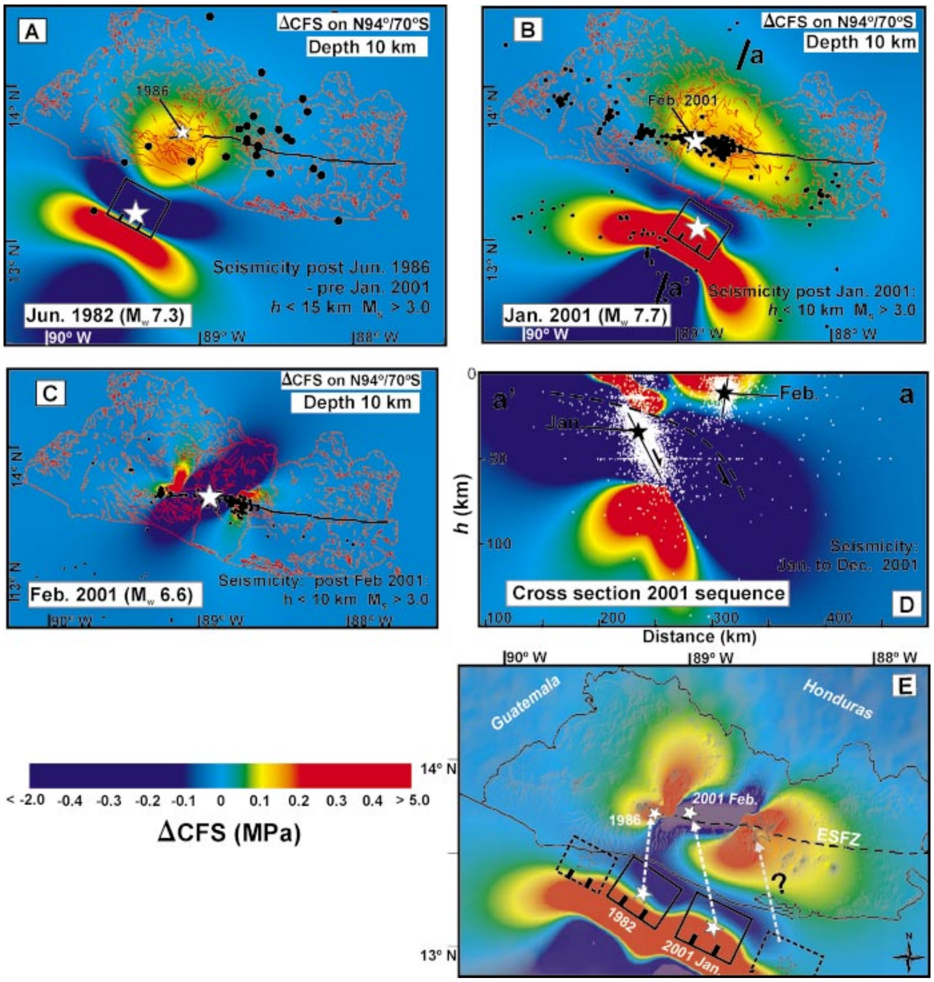

Figure 4. A–C: Models of change in static Coulomb failure stress (CFS) generated after events of 1982, January 2001, and February 2001 projected on map of faults. Black line represents El Salvador fault zone (ESFZ). D: Model for 2001 event is shown in cross section. E: Joint model with CFS change generated by three major events. Rectangles represent surface ruptures. Dotted rectangles represent hypothetical ruptures.

essary in order to obtain a more realistic map of static CFS change. It will also be necessary to take into account the effect of transitory dynamic CFS changes in order to analyze the 2001 earthquakes that were separated by only one month. Dynamic stress changes associated with the passage of seismic waves have been proposed to explain the remote seismicity that occurred within the several months following a large earthquake (Kilb et al., 2000). In any case, both the history of the large earthquakes in El Salvador and the local geologic structure give enough evidence to support the existence of static stress triggering processes in the area.

The El Salvador fault zone east of the Rio Lempa was stressed by the 2001 earthquakes. The likelihood of rupture is thus increased in this area. However, no available information exists on the past rupture history of this fault. Further studies are necessary to constrain the controlling factors for hazard (recurrence interval and elapsed time since the last rupture) and to combine them with the results of this study.

ACKNOWLEDGMENTS

This research has been financed by the Spanish Agency of International Cooperation and the project Ren2001-0266-C02-02. We thank S. Prejean and T. Parsons for helpful reviews and B.A. van der Pluijm for helpful review comments We are grateful to R. Robinson for his permission to use the software GNStress. We also thank J. Rodriguez and J. Jimenez, who helped with the use of the geographic information system.

REFERENCES CITED

Benito, B., Cepeda, J., and Martínez-Díaz, J.J., 2004, Analysis of the spatial and temporal distribution of the 2001 earthquakes, *in* Rose, W.I., et al., eds., Recent work on natural hazards mitigation in El Salvador: Geological Society of America Special Paper 375 (in press).

Bommer, J., Benito, B., Ciudad-Real, M., Lemoine, A., López-Menjivar, M., Madariaga, R., Mankelow, J., Mendez-Hasbun, P., Murphy, W., Nieto-Lovo, M., Rodríguez, C., and Rosa, H., 2002, The Salvador earthquakes of January and February 2001: Context, characteristics and implications for seismic risk: Soil Dynamics and Earthquake Engineering, v. 22, p. 389–418.

Bosse, H.R., Lorenz, W., Merino, A., Mihm, A., Rode, K., Schmidt-Thomé, M., Wiesemann, G., and Weber, H.S., 1978, Geological map of El Salvador Republic: Hannover, Germany, Bundesanstalt für Geowissenschaften und Rohstoffe, D-3, scale 1:100,000.

Buforn, E., Lemoine, A., Udias, A., and Madariaga, R., 2001, Mecanismo focal de los terremotos de El Salvador, *in* Martínez-Guevara, J.M., ed., Memorias 2nd Congreso Iberoamericano de Ingeniería Sísmica, Madrid, Spain: p. 115–118.

DeMets, C., 2001, A new estimate for present-day Cocos-Caribbean plate motion: Implications for slip along the Central American volcanic arc: Geophysical Research Letters, v. 28, p. 4043–4046.

Deng, J., and Sykes, L.R., 1997, Stress evolution in southern California and triggering of moderate-, small-, and micro-sized earthquakes: Journal of Geophysical Research, v. 102, p. 411–435.

Dewey, J.W., and Suarez, G., 1991, Seismotectonics of Middle America, *in* Slemmons, D.B., et al., eds., Neotectonics of North America: Boulder, Colorado, Geological Society of America, Geology of North America, Decade map volume, p. 309–321.

Harlow, D.H., and White, R.A., 1985, Shallow earthquakes along the volcanic chain in Central America: Evidence for oblique subduction: Earthquake Notes, v. 55, p. 28.

Harris, R.A., 1998, Introduction to special section: Stress triggers, stress shadows, and implications for seismic hazard: Journal of Geophysical Research, v. 103, p. 347–358.

Isacks, B., and Baranzagi, M., 1977, Geometry of Benioff zones: Lateral segmentation and downwards bending of the subducted lithosphere, *in* Talwani, M., and Pitman, W.C., eds., Island arcs, deep sea trenches, and back-arc basins: American Geophysical Union Maurice Ewing Series, v. 1, p. 99–114.

Kilb, D., Gomberg, J., and Bodin, P., 2000, Earthquake triggering by dynamic stresses: Nature, v. 408, p. 570–574.

King, G.C.P., Stein, R.S., and Lin, J., 1994, Static stress changes and the triggering of earthquakes: Seismological Society of America Bulletin, v. 84, p. 935–953.

Okada, Y., 1992, Internal deformation due to shear and tensile faults in a half space: Seismological Society of America Bulletin, v. 82, p. 1018–1040.

Parsons, T., 2002, Global Omori-law decay of triggered earthquakes: Large aftershocks outside the classical aftershock zone: Journal of Geophysical Research, v. 107, 2199, DOI 10.1029/2001JB000646.

Stein, R.S., 1999, The role of stress transfer in earthquake recurrence: Nature, v. 402, p. 605–609.

Vallée, M., and Bouchon, M., 2003, The 13 January 2001 El Salvador earthquake: A multidata analysis: Journal of Geophysical Research, v. 108, 2203, DOI 10.102972002JB001922.

Wells, D.L., and Coppersmith, K.J., 1994, New empirical relations among magnitude, rupture length, rupture width, rupture area and surface displacement: Seismological Society of America Bulletin, v. 85, p. 1–16.

White, R., 1991, Tectonic implications of upper-crustal seismicity in Central America, *in* Slemmons, D.B., et al., eds., Neotectonics of North Amercia: Boulder, Colorado, Geological Society of America, Geology of North America, Decade map volume, p. 323–338.

White, R.A., and Harlow, D.H., 1993, Destructive upper-crustal earthquakes of Central America since 1900: Seismological Society of America Bulletin, v. 83, p. 1115–1142.

White, R.A., Harlow, D.H., and Álvarez, S., 1987, The San Salvador earthquake of October 10, 1986: Seismological aspects and other recent local seismicity: Earthquake Spectra, v. 3, p. 419–434.

Manuscript received 2 August 2003
Revised manuscript received 1 October 2003
Manuscript accepted 2 October 2003

Printed in USA